General Disclaimer

One or more of the Following Statements may affect this Document

- This document has been reproduced from the best copy furnished by the organizational source. It is being released in the interest of making available as much information as possible.

- This document may contain data, which exceeds the sheet parameters. It was furnished in this condition by the organizational source and is the best copy available.

- This document may contain tone-on-tone or color graphs, charts and/or pictures, which have been reproduced in black and white.

- This document is paginated as submitted by the original source.

- Portions of this document are not fully legible due to the historical nature of some of the material. However, it is the best reproduction available from the original submission.

NATIONAL AERONAUTICS AND SPACE ADMINISTRATION

Technical Report 32-1601

New Optical and Radio Frequency Angular Tropospheric Refraction Models for Deep Space Applications

Allen L. Berman

Stephen T. Rockwell

JET PROPULSION LABORATORY
CALIFORNIA INSTITUTE OF TECHNOLOGY
PASADENA, CALIFORNIA

November 1, 1975

NATIONAL AERONAUTICS AND SPACE ADMINISTRATION

Technical Report 32-1601

New Optical and Radio Frequency Angular Tropospheric Refraction Models for Deep Space Applications
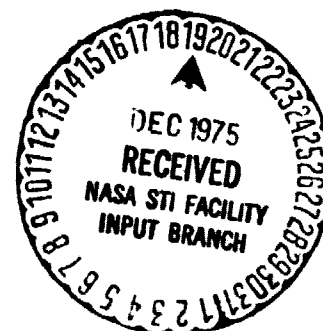
Allen L. Berman
Stephen T. Rockwell

JET PROPULSION LABORATORY
CALIFORNIA INSTITUTE OF TECHNOLOGY
PASADENA, CALIFORNIA

November 1, 1975

Preface

The work described in this report was performed by the DSN Operations Division of the Jet Propulsion Laboratory.

Contents

PRECEDING PAGE BLANK NOT FILMED

Contents (contd)

Tables

Figures

Abstract

This report presents the development of angular tropospheric refraction models for optical and radio frequency usage. The models are compact analytic functions, finite over the entire domain of elevation angle, and accurate over large ranges of pressure, temperature, and relative humidity. Additionally, FORTRAN subroutines for each of the models are included.

New Optical and Radio Frequency Angular Tropospheric Refraction Models for Deep Space Applications

I. Introduction

There exists here at the Jet Propulsion Laboratory (JPL), and particularly within the Deep Space Network (DSN), a need for accurate, yet modestly sized, optical and radio frequency (RF) angular tropospheric refraction models. The basic angular refraction model (and several close variants) currently in use at JPL consists of three radically different analytic functions, each applicable over a different range of zenith angle (zenith angle = 90° − elevation angle) and is therefore immediately rather cumbersome. Furthermore, the accuracy of the current JPL refraction model is not well documented, and is thus subject to considerable doubt.

The present time is particularly well suited to reexamine the question of an angular refraction model for the following reasons:

(1) The remote site Antenna Pointing Subsystem (APS) is currently being redesigned, thus affording the capability to easily change the angular refraction modeling.

(2) The recent advent of X-band capability, with an antenna beamwidth of approximately 0.020°, has underscored the need for high-accuracy angular predicts.

The angular refraction model (or variants thereof) currently in use at JPL is as follows:

(1) For $Z \leq 80.26°$,

$$R = (N/10^6) \tan Z$$

(2) For $90° \geq Z > 80.26°$,

$$R = \left(\frac{N}{340}\right)\left(\frac{0.0007}{0.0589 + \left(\frac{\pi}{2} - Z^{\bullet}\right)} - 0.00126\right)$$

(3) For $Z > 90°$,

$$R = \left(\frac{\pi}{180}\right)\left(0.60874 - 0.201775\left\{\frac{180}{\pi}\right\}\left[Z^{\bullet} - \frac{\pi}{2}\right]\right)$$

where

R = refraction correction, rad

Z = zenith angle (actual), deg

$Z^{\bullet}$ = zenith angle (actual), rad

N = "refractivity"

To gauge the degree of error inherent to the current JPL refraction model, it has been contrasted to a con-

tinuous set of refraction data as computed from the work of B. Garfinkel (see Refs. 1 and 2), and is seen in Fig. 1. The Garfinkel data is for pressure $P = 760$ mm of Hg and temperature $T = 0°C$; the JPL model data has been matched to these conditions by setting $N = 288$ (i.e., additionally assuming relative humidity RH = 0.0%). The most distressingly obvious flaws in the current JPL model are the discontinuities in R at the two breakpoints, these discontinuities (and hence errors in one or the other segment) amounting to approximately 30 and 300 arc seconds (sec), respectively. (Note: For the duration of this report, refraction quantities will be dealt with in terms of arc seconds, with $0.001° = 3.6$ sec.) Further examination of the current model discloses that the first two segments are dependent upon the "refractivity" N, and hence pressure and temperature, while the third segment is not. Given that the current JPL model is inaccurate, has very large discontinuities at the segment breakpoints, and is fundamentally cumbersome because of the tri-segment construction, it would seem to be a likely candidate for a more accurate and reasonable replacement.

The approach adopted here will be to construct first a very accurate optical angular refraction model of the form

$$R_{oP} = R_{oP}(P,T,Z)$$

and then translate these results to the radio frequency case by explicitly defining a function of f such that:

$$R_{RF} = R_{oP}(P,T,Z)\{f(P,T,RH)\}$$

Section II will generate the optical refraction model, while Section III will construct the RF refraction model.

II. A New Optical Angular Refraction Model

A. General Approach to a New Optical Angular Refraction Model

In the previous section, the undesirability of the current JPL angular refraction model was demonstrated; in this section the general philosophy used to generate a new optical angular refraction model will be dealt with. One starts with the fact that angular refraction is crucially important in the effectuation of various astronomical endeavors, and hence there exists copious amounts of refraction data. The main drawback to these data is, however, that they are either in tabular form or are calculated via schemes which require large amounts of tabular inputs

(for instance, see Refs. 1, 2, 3, and 4). Furthermore, the astronomical accuracy requirements are very stringent (perhaps down to about the 1-sec level), while the DSN requirements are no greater than the 10-sec level. In light of the above, it is clear that one reasonable approach would be to use empirical methods to develop a simple analytical expression to approximate the very accurate astronomical refraction data available. Since the envisioned use of the new model within the DSN includes small remote site computers as well as large central complex computers, desirable features would include:

(1) A single expression over the entire domain of Z, instead of multiple segments, each applicable over different ranges of Z.

(2) Accuracy to about the 10-sec level for reasonable ranges of Z and tropospheric conditions.

(3) Model to be designed to minimize both computer memory and run time.

B. Selection of an Optical Angular Refraction Data Base

After a review of the literature, it became apparent that a reasonable selection for a data base would be the work of Boris Garfinkel of the Yale University Observatory (see Refs. 1 and 2). Garfinkel's original theory was published in 1944, and then reexamined in 1966. The form of his model is semi-analytical in that it is a closed function with Z, P, T as variables, but also requires tabular input in the form of Z-dependent polynomial coefficients. More importantly, his model is continued for $Z > 90°$, an aspect which is most frequently missing in other angular refraction works. Finally his work compares well with other authorities in the field. For instance, Garfinkel compares his data at $P = 760$ mm and $T = 0°C$ with those of the Radau and the Pulkova models as follows (with Z' (observed zenith angle) in degrees and R in seconds):

Z'	R Garfinkel	R Radau	R Pulkova
80	331	331	331
81	368	366	365
82	410	409	408
83	466	462	460
84	531	529	527
85	619	617	614
86	738	735	733
87	905	903	900
88	1153	1152	1147
89	1544	1545	1537
90	2206	2208	2199

Table 1 provides a detailed tabulation of Garfinkel refraction data for $0° \leq Z \leq 93°$, $P = 760$ mm, and $T = 0°C$.

C. Derivation of a Basic Optical Angular Refraction Model

The needs of the DSN for an angular refraction model are restricted to the following range of Z':

$$0° \leq Z' \lesssim 92°$$

where

$$Z' = Z - R(Z) = \text{observed zenith angle}$$

this range being encompassed by the Garfinkel data in Table 1. It was hoped that the data base chosen (i.e., the Garfinkel data whose selection was discussed in the previous Subsection) could be approximately fit to a function (or functions, as necessary) via routine least squares techniques. It was planned to do all work for $P = 760$ mm and $T = 0°C$ under the assumption that P and $\dot{T}$ effects could be (multiplicatively) added at a subsequent time. The data base chosen was a slightly smaller subset of the data base displayed in Table 1. The frequency of data points was rather arbitrarily chosen as follows:

Range of Z, deg	Data frequency, deg
$0 \leq Z \leq 70$	0.5
$70 \leq Z \leq 85$	0.2
$85 \leq Z \leq 93$	0.1

with the net effect that the refraction data were increasingly "weighted" in the high Z region where the rate of change of refraction is the greatest. The computer program utilized in this study is a standardized least squares subroutine available to all UNIVAC 1108 users at JPL (see Ref. 5). Basically, it fits a data set to an nth degree polynomial such that the residuals are minimized in a least squares sense, i.e.,

$$\text{if} \quad R_i(Z_i); \quad i = \text{data set}$$

then a function X is formulated such that

$$X = \sum_{j=0}^{n} K_{j+3} \{U(Z)\}^j$$

where

$$K_1 = \frac{1}{2} [(R_i)_{max} + (R_i)_{min}]$$

$$K_2 = \frac{1}{2} [(R_i)_{max} - (R_i)_{min}]$$

$$U(Z) = \frac{1}{K_2} [Z - K_1]$$

and where the conditions satisfied are the following $n + 1$ equations in $n + 1$ unknowns.

Let

$$\Delta_i = R_i(Z_i) - X(Z_i)$$

$$\sigma = \left[\sum^{i} \Delta_i^2 \right]^{1/2}$$

Then, finally,

$$\frac{\partial \sigma}{\partial K_3} = 0$$

$$\frac{\partial \sigma}{\partial K_4} = 0$$

.

.

.

$$\frac{\partial \sigma}{\partial K_{n+3}} = 0$$

It was originally intended to attempt a least squares curve fit to the "raw" refraction data, shown in Fig. 2. It was observed, however, that the natural log (ln) of R gave a very smooth representation and possessed, of course, far less dynamic range, as can be seen in Fig. 3. It seemed possible that it might yield a better fit for a lower order polynomial (a desirable property), i.e., fitting:

$$\ln (R_i(Z_i)); \quad X$$

Finally, it was observed that taking the inverse tangent (arctan) of ln (R) yielded a representation that appeared almost linear, as can be seen in Fig. 4. This was also felt to be worth attempting as a fit, in the form of:

$$\arctan \left\{ \frac{\ln (R_i(Z_i))}{\ln (R(45°))} \right\}; \quad X$$

The ln (R) fit was attempted first as the most likely candidate. The main goal established was to find the smallest order fit which would keep the maximum residual below some reasonable limit. The results of a series of different order fits appear in Fig. 5. Although it might at first seem strange that the absolute maximum residual does not decrease monotonically with degree of fit, all one should really expect is that σ decrease monotonically with degree of fit, and this was the case. At any rate, the 8th degree case was felt to be the best compromise, as one needed to go to a 14th degree fit to obtain significant improvement. The other two types of fits were attempted, with a general tradeoff expected that an increase in functional dependence (ln, arctan, etc.) should decrease the order of fit necessary. A few of the salient features of each of the three types of fits attempted are:

(1) Raw Data Fit

    (a) Simple—no additional functions required for modeling.

    (b) Minimum acceptable polynomial required ~12th order.

    (c) Large residuals (~20 sec or higher) as $Z \rightarrow 0°$, leading to unpalatable result of refraction being applied in wrong direction at very small Z, etc.

(2) Ln(R) Fit

    (a) Model would require natural exponentiation (exp).

    (b) Minimum acceptable polynomial required ~8th order.

    (c) Logarithmic condition of fit forces residuals to be approximately proportional to R, so residuals quite small except at very large Z.

(3) Arctan (ln(R)) Fit

    (a) Model would require tangent (tan) and exp.

    (b) Minimum polynomial fit required ~6th order.

    (c) Extremely low residuals for $Z \lesssim 90°$ and quite high residuals for $Z \gtrsim 90°$.

A comparison of the three types of fits is seen in Fig. 6.[1] The ln R fit was assessed to be the best compromise

---

[1]This figure and Figs. 7, 9, and 10 were prepared on the basis of interim results and are at variance with the final model by as much as 5 sec at large Z. Therefore, they should be used for illustration only.

amongst the design goals stated in Subsection A. **Further refinement to the 8th order ln R fit** was accomplished by making minor adjustments to the data set used in the fit process, until an optimum fit (in the sense of the smallest maximum residual) was achieved. For this case, the maximum residual in the interval $0° \leq Z \leq 92°$ occurred at about $Z = 91.1°$ and had a value of:

$$\Delta R = +21.6 \text{ sec}$$

D. Complete Optical Refraction Model Determination

The refraction model, as finally determined in the previous section, is as follows:

$$R = \exp\left\{ \sum_{j=0}^{8} K_{j+3}\,[U(Z)]^j \right\} - K_{12}$$

where

$$\bar{R} = \text{refraction, sec}$$
$$Z = \text{zenith angle, actual}$$
$$EL = 90° - Z = \text{elevation angle}$$
$$U(Z) = \left\{ \frac{Z - K_1}{K_2} \right\}$$
$$K_1 = 46.625$$
$$K_2 = 45.375$$
$$K_3 = 4.1572$$
$$K_4 = 1.4468$$
$$K_5 = 0.25391$$
$$K_6 = 2.2716$$
$$K_7 = -1.3465$$
$$K_8 = -4.3877$$
$$K_9 = 3.1484$$
$$K_{10} = 4.5201$$
$$K_{11} = -1.8982$$
$$K_{12} = 0.89000$$

When this model is compared to the Garfinkel data (with $P = 760$ mm and $T = 0°C$), the following maximum residuals[2] result:

$$0° \leq Z \leq 85° \qquad \Delta R = + \quad 5.6 \text{ sec}$$

---

[2]All residuals (ΔR) will be Garfinkel Data — Proposed Model.

$$85° \leq Z \leq 92° \qquad \Delta R = + \ 21.6 \ \text{sec}$$

$$92° \leq Z \leq 93° \qquad \Delta R = -302.6 \ \text{sec}$$

The very large residuals between $Z = 92°$ and $Z = 93°$ are primarily a result of ending the fit at $92°$. At this point there was still one point of concern and that was:

$$\text{As } Z > 93°$$

$$|R| \rightarrow \text{very large}$$

such that at some $Z > 93°$ there exists the following condition:

$$Z - R(Z) < 90° \ (\text{or local horizon})$$

giving the appearance of a "false" rise. This would, of course, pose difficulties for trajectory-type programs which calculate, and examine for a rise condition, zenith angles considerably larger than $90°$. Based on this undesirable feature, it was felt that the model should be modified such that shortly after $Z = 93°$ it would be required that:

$$R(Z) \rightarrow 0$$

At the same time, it was felt that possibly the characteristics of the model for $Z \gtrsim 90°$ could be improved upon. The residuals between $Z = 90°$ and $Z = 93°$ look like:
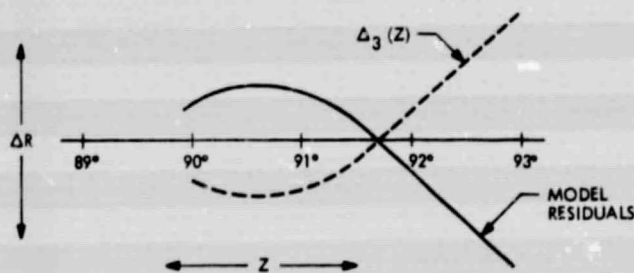
It was therefore felt that if a function (say, $\Delta_3(Z)$) could be derived with inverse characteristics to the above residuals plus possessing the following qualities:

$$\Delta_3(Z) \rightarrow \text{very large for } Z \gtrsim 93°$$

$$\Delta_3(Z) \rightarrow \text{very small for } Z \lesssim 90°$$

then a model of the form:

$$R = \exp\left\{ \left(\sum_{j=0}^{8} K_{j+3} [U(Z)]^j \right) \Big/ [1 + \Delta_3(Z)] \right\} - K_{12}$$

could perhaps both improve the present model between $90°$ and $93°$ and drive the model to approximately zero (actually $1 - K_{12}$) thereafter. A function to accomplish this was constructed (empirically) as follows:

$$\Delta_3(Z) = (Z - C_0) \{\exp [C_1(Z - C_2)]\}$$

where

$$Z = \text{zenith angle, deg}$$

$$C_0 = 91.870$$

$$C_1 = 0.80000$$

$$C_2 = 99.344$$

The improvement in the $Z = 90°$ to $Z = 93°$ region can be seen in Fig. 7, while the rapid drop off of the modified model after $Z = 93°$ can be viewed in Fig. 8. The maximum residuals after the above modification become:

$$0° \leq Z \leq 85° \qquad \Delta R = + \ 5.6 \ \text{sec}$$

$$85° \leq Z \leq 92° \qquad \Delta R = -14.7 \ \text{sec}$$

$$92° \leq Z \leq 93° \qquad \Delta R = -15.0 \ \text{sec}$$

E. Refraction Model Functional Dependence Upon Pressure, Temperature, and Relative Humidity

It was originally felt that once a refraction model for standard conditions ($P = 760$ mm and $T = 0°$C) had been achieved, the usual scaling by $P/760$ and $273/(T + 273)$ could be applied. However, after examining different combinations of P and T in the Garfinkel data, this did not prove to be an adequate treatment of the pressure and temperature dependence, and additional work in this area was required.

1. **Pressure correction.** Examination of the Garfinkel data at different pressures indicated that scaling of the basic model by $P/760$ was reasonable at most Z, but broke down as $Z \gtrsim 90°$. It was hoped that this could be compensated for by a correction factor (say, $\Delta_1(P, Z)$) such that the entire pressure correction factor would be of the form:

$$\frac{P}{760} \{1 - \Delta_1(P, Z)\}$$

Furthermore, it would be necessary that:

$$\Delta_1(P, Z) \to 0, \quad Z \lesssim 90°$$

$$\Delta_1(P, Z) \to 0, \quad Z \gtrsim 93°$$

It was noted in the examination of the Garfinkel data that the pressure effect (as different from $P/760$) was for the most part separable, i.e.:

$$\Delta_1(P, Z) \sim \Delta_p(P)\Delta_z(Z)$$

and it could be seen that further:

$$\Delta_p(P) \sim (P - 760)$$

A representation for Δ_z was then empirically constructed as follows:

$$\Delta_z(Z) \sim \exp[A_1(Z - A_2)]$$

so that the $\Delta_1(P, Z)$ pressure correction would be:

$$\Delta_1(P, Z) = (P - 760) \exp[A_1(Z - A_2)]$$

The results of using $\Delta_1(P, Z)$, above, can be seen in Fig. 9. Finally, to satisfy the conditions of a small $\Delta_1(P, Z)$ for $Z \gtrsim 93°$, the previously determined $\Delta_3(Z)$ was utilized to arrive at the following expression:

Pressure correction factor =

$$\frac{P}{760}\left\{1 - \frac{(P - 760)\exp[A_1(Z - A_2)]}{1 + \Delta_3(Z)}\right\}$$

where

Z = zenith angle, deg

P = pressure, mm of Hg

$A_1 = 0.40816$

$A_2 = 112.30$

$\Delta_3(Z)$ = as previously defined

2. Temperature correction. The investigation of temperature effects proceeded along the same lines as the investigation of pressure effects in the previous section, with the goal of a total temperature correction factor in the form of:

$$\frac{273}{T + 273}\{1 - \Delta_2(T, Z)\}$$

in combination with the conditions:

$$\Delta_2(T, Z) \to 0 \quad Z \lesssim 90°$$

$$\Delta_2(T, Z) \to 0, \quad Z \gtrsim 93°$$

Similarly, the temperature effect was found to be approximately separable:

$$\Delta_2(T, Z) \sim \Delta_t(T)\Delta_z(Z)$$

and the following was (empirically, constructed:

$$\Delta_t \sim T$$

$$\Delta_z \sim \exp[B_1(Z - B_2)]$$

so that the $\Delta_2(T, Z)$ temperature correction would be:

$$\Delta_2(T, Z) = (T)\exp[B_1(Z - B_2)]$$

The results of using $\Delta_2(T, Z)$, above, are seen in Fig. 10. Once again, to satisfy the condition of a small $\Delta_2(T, Z)$ for $Z \gtrsim 93°$, the previously determined $\Delta_3(Z)$ is utilized to arrive at the following total expression:

Temperature correction factor =

$$\frac{273}{T + 273}\left\{1 - \frac{(T)\exp[B_1(Z - B_2)]}{1 + \Delta_3(Z)}\right\}$$

where

Z = zenith angle, deg

T = temperature, °C

$B_1 = 0.12820$

$B_2 = 142.88$

$\Delta_3(Z)$ = as previously determined

3. Relative humidity correction. Both Garfinkel (see Ref. 2) and the Pulkova Model (see Ref. 4) indicate that the correction for relative humidity is very small, perhaps on the order of several seconds at large Z, at a maximum. It was therefore decided here to ignore corrections based on relative humidity, at least until some time when a stronger case can be made for the necessity of its inclusion, given the level of accuracy (10 sec) inherent to the model here being proposed.

F. Complete Optical Angular Refraction With Pressure and Temperature Corrections

The final refraction model with pressure and temperature accounted for is as follows:

$$R = F_p F_t \left(\exp \left\{ \frac{\sum_{j=0}^{8} K_{j+3} [U(Z)]^j}{1 + \Delta_3(Z)} \right\} - K_{12} \right)$$

$$F_p = \left(\frac{P}{P_0} \left\{ 1 - \frac{\Delta_1(P, Z)}{1 + \Delta_3(Z)} \right\} \right)$$

$$F_t = \left(\frac{T_0}{T} \left\{ 1 - \frac{\Delta_2(T, Z)}{1 + \Delta_3(Z)} \right\} \right)$$

$$\Delta_1(P, Z) = (P - P_0)\{\exp[A_1(Z - A_2)]\}$$

$$\Delta_2(T, Z) = (T - T_0)\{\exp[B_1(Z - B_2)]\}$$

$$\Delta_3(Z) = (Z - C_0)\{\exp[C_1(Z - C_2)]\}$$

where

R = refraction, sec

Z = actual zenith angle, deg

$EL = 90° - Z$ = elevation angle

$$U(Z) = \left\{ \frac{Z - K_1}{K_2} \right\}$$

$K_1 = 46.625$

$K_2 = 45.375$

$K_3 = 4.1572$

$K_4 = 1.4468$

$K_5 = 0.25391$

$K_6 = 2.2716$

$K_7 = -1.3465$

$K_8 = -4.3877$

$K_9 = 3.1484$

$K_{10} = 4.5201$

$K_{11} = -1.8982$

$K_{12} = 0.89000$

P = pressure, mm of Hg

$P_0 = 760.00$ mm

$A_1 = 0.40816$

$A_2 = 112.30$

T = temperature, K

$T_0 = 273.00$ K

$B_1 = 0.12820$

$B_2 = 142.88$

$C_0 = 91.870$

$C_1 = 0.80000$

$C_2 = 99.344$

The accuracy of this model for various pressures, temperatures, and ranges of Z, as compared to the Garfinkel data, can be seen in Table 2.

The signature of the residuals at large Z and with $P = 760$ mm and $T = 0°C$ can be seen in Fig. 7 (modified 8th order ln R fit). For use where simplicity is of a more urgent need than accuracy, an abbreviated version of the model can be obtained by setting:

$$\Delta_1 = \Delta_2 = \Delta_3 = 0$$

such that one has:

$$R = \left(\frac{P}{P_0} \right) \left(\frac{T_0}{T} \right) \left(\exp \left\{ \sum_{j=0}^{8} K_{j+3} [U(Z)]^j \right\} - K_{12} \right)$$

where all quantities are as previously defined. The accuracy of this abbreviated version, once again as compared to the Garfinkel data, is seen in Table 3. Also, the effects of the deletion of Δ_1 is seen in Fig. 9, of Δ_2 in Fig. 10, and of Δ_3 in Fig. 7.

G. FORTRAN Subroutines of the Optical Refraction Models

Appendix A presents a FORTRAN subroutine of the full model described in Subsection F, while Appendix B presents a FORTRAN subroutine corresponding to the abbreviated model, also described in Subsection F. Inputs required are as follows:

PRESS = pressure, mm of Hg

TEMP = temperature, K

ZNITH = actual zenith angle, deg

and the subroutine(s) return with:

$$R = \text{refraction correction, sec}$$

III. A New Radio Frequency Angular Refraction Model

In the previous section, a new optical angular refraction model was presented. In this section, past attempts to translate from an optical model to a radio frequency model will be dealt with, and then a new method to accomplish this transformation will be proposed.

A. Past Attempts to Transform Angular Refraction Models From Optical to Radio Frequencies

To facilitate a discussion of past attempts to generate angular tropospheric refraction models for use at radio frequencies, let the following notation be introduced:

$R_{OP} = R(P,T,Z) = $ optical refraction model from section II

$R_{RF} = R_{RF}(P,T,Z,RH) = $ radio frequency refraction model

$P = $ pressure

$T = $ temperature

$Z = $ zenith angle

$RH = $ relative humidity

$N(h) = ND(h) + NW(h)$

$N(h) = $ total refractivity at radio frequencies

$ND(h) = $ dry, or optical component, of refractivity

$NW(h) = $ wet component of refractivity

$h = $ height

$h_0 = $ station height

$s = $ parameter surface value

$ND(h_0) = ND_s$

$NW(h_0) = NW_s$

$N(h_0) = N_s$

In general, attempts to construct a radio frequency refraction model consisted of appropriating an empirical model from optical refraction work which would give the functional dependence on Z (say $R_Z(Z)$), and then scaling

this expression by the total radio frequency surface refractivity, i.e.,

$$\text{refraction} \approx \left(\frac{N_s}{N_R}\right) R_Z(Z)$$

where $N_R = $ reference optical refractivity.

At this point, one must ask, what are the implications of this procedure? Since any signal (that is of interest here) must traverse the entire troposphere, and is of course, continually being refracted, one might think that instead of being proportional to surface refractivity, angular refraction is really more nearly proportional to total (integrated) tropospheric refractivity, i.e.,

$$\text{refraction} \propto \int N(h)\, dh$$

However, refraction could also be proportional to surface refractivity if it could be assumed that there exists some $f(h)$ such that:

$$N(h) \approx N_s f(h)$$

so that

$$\text{refraction} \propto \int N_s f(h)\, dh = N_s \int f(h)\, dh$$

Making the assumption that

$$ND(h) \sim ND_s f_1(h)$$

$$NW(h) \sim NW_s f_2(h)$$

one would have for the optical case:

$$R_Z \propto \int ND(h)\, dh = \int ND_s f_1(h)\, dh$$
$$= ND_s \int f_1(h)\, dh$$

For the radio frequency case:

$$R_{RF} \propto \int N(h)\, dh = \int \{ND(h) + NW(h)\}\, dh$$
$$= \int \{ND_s f_1(h) + NW_s f_2(h)\}\, dh$$
$$= ND_s \int f_1(h)\, dh + NW_s \int f_2(h)\, dh$$

Without precise knowledge of the form of $f_1(h)$ and $f_2(h)$, the only way that the surface refractivities could be used to transform from the optical case to the radio case would be if

$$f_1(h) \approx f_2(h)$$

Then

$$R_{RF} \propto (ND_s + NW_s) \int f_1(h)\, dh$$

and indeed

$$R_{RF} \propto (ND_s + NW_s)\left[\frac{R_z(Z)}{ND_s}\right]$$

However, it is well known that wet refractivity "decays" much more rapidly than dry refractivity (for instance, Ref. 6), so that $f_1(h)$ and $f_2(h)$ are quite dissimilar; thus, the procedure of scaling an optical angular refraction model by the total surface radio refractivity to achieve a radio angular refraction model would appear to be seriously flawed.

B. Method Used to Transform From an Optical to a Radio Frequency Refraction Model

From the previous section it was seen that

$$R_{RF} \propto N_s = ND_s + NW_s$$

is a poor choice. A more logical choice would be

$$
\begin{aligned}
R_{RF} \propto \int N(h)\, dh &= \int \{ND(h) + NW(h)\}\, dh \\
&= \int ND(h)\, dh + \int NW(h)\, dh \\
&= \int ND(h)\, dh \left\{ 1 + \frac{\int NW(h)\, dh}{\int ND(h)\, dh} \right\}
\end{aligned}
$$

Similarly, for the optical case (using the model previously presented):

$$R_{OP} \propto \int ND(h)\, dh$$

Combining the above, one arrives at the equation that will be used for the radio frequency angular refraction model:

$$R_{RF}(P,T,Z,RH) \approx R_{OP}(P,T,Z)\left\{ 1 + \frac{\int NW(h)\, dh}{\int ND(h)\, dh} \right\}$$

C. Determination of Ratio of Integrated Wet Refractivity to Integrated Dry Refractivity

In attempting to determine an analytical parametric representation for the expression:

$$\frac{\int NW(h)\, dh}{\int ND(h)\, dh}$$

the most difficult problem by far lies with the integrated wet refractivity. Berman first showed in 1970 (Ref. 7) that

$$\int ND(h)\, dh = AP_s\left[\frac{R}{g}\right]$$

where

$A = 77.6$

$P_s = $ surface pressure, mbar

$R = $ perfect gas constant

$g = $ gravitational acceleration

$g/R = 34.1\,^\circ\text{C/km}$

and also gave an expression to approximate the integrated wet refractivity:

$$\int NW(h)\, dh =$$

$$\left[\frac{C_1 C_2 (RH)_s}{\gamma}\right]\left\{ \frac{\left(1 - \dfrac{C}{T_0}\right)^2}{B - AC} \right\} \exp\left(\frac{AT_0 - B}{T_0 - C}\right)$$

where

$C_1 = 77.6$

$C_2 = 29341.0$

$RH = $ relative humidity

$\gamma = $ temperature lapse rate

$C = 38.45$

$T_0 = $ extrapolated surface temperature

$A = 7.4475 \ln(10)$

$B = 2034.28 \ln(10)$

Chao (Ref. 8) later improved upon the integrated wet refractivity with the expression:

$$\int NW(h)\, dh = 1.63 \times 10^2 \left\{ \frac{e_0^{1.23}}{T_0^2} \right\} + 2.05 \times 10^2\, \alpha \left\{ \frac{e_0^{1.46}}{T_0^3} \right\}$$

where

$e_0 = $ surface vapor pressure, N/m^2

$T_0 = $ surface temperature, K

$\alpha = $ temperature lapse rate, K/km

However, both of these expressions depend upon one or more parameters not measurable at the surface (i.e., temperature lapse rate, etc.), and neither is particularly accurate. Going back to the previous section, if the altitude-dependent refractivities could really be represented as

$$ND(h) \sim ND_s f_1(h)$$

$$NW(h) \sim NW_s f_2(h)$$

and if the above refractivities could be integrated, i.e., if A below could be evaluated as

$$A = \frac{\int f_2(h)\,dh}{\int f_1(h)\,dh}$$

then one might simply expect that

$$\frac{\int NW(h)\,dh}{\int ND(h)\,dh} \approx A \left\{ \frac{NW_s}{ND_s} \right\}$$

To test this hypothesis, the authors had ten cases used in Ref. 7. Although a very small number, the cases were alternate day and night profiles selected throughout the year (December, February, April, August, September). A least-squares linear curve fit to the above data was performed as follows:

$$\frac{\int NW(h)\,dh}{\int ND(h)\,dh} ; \qquad A \left\{ \frac{NW_s}{ND_s} \right\}$$

The fit yielded the following:

$$A = 0.3224$$

$$\sigma(\%) = 00.93\%$$

$$\sigma(\%) = 100 \times \sigma \left(\frac{\int NW(h)\,dh}{\int ND(h)\,dh} - A \left\{ \frac{NW_s}{ND_s} \right\} \right)$$

Translated to centimeters of integrated refractivity, one would have

$$\sigma(\text{cm}) = 2.0\,\text{cm}$$

Table 4 and Fig. 11 present the detailed analysis of the ten cases described.

As a totally independent check of this observed relationship, use can be made of work done by Chao (Ref. 6) on wet and dry refractivity profiles. Combining Eqs. (9), (10), (13), (14), (15), and (16) from Ref. 6 one has:

$$ND(h) = ND_s \left(1 - \frac{h}{42.7} \right)^4 \qquad h \leq 12.2\,\text{km}$$

$$= \frac{70}{269} ND_s \left\{ \exp\left(-\frac{(h - 12.2)}{6.4} \right) \right\} \qquad h \geq 12.2\,\text{km}$$

$$NW(h) = NW_s \left(1 - \frac{h}{13} \right)^4 \qquad h \leq 13\,\text{km}$$

$$= 0 \qquad h \geq 13\,\text{km}$$

Performing the dry refractivity integration, one has

$$\int_0^\infty ND(h)\,dh = \int_0^{12.2} ND_s \left(1 - \frac{h}{42.7} \right)^4 dh$$

$$+ \int_{12.2}^\infty \frac{70}{269} ND_s \left\{ \exp\left(-\frac{(h - 12.2)}{6.4} \right) \right\} dh$$

$$= ND_s \int_0^{12.2} \left(1 - \frac{h}{42.7} \right)^4 dh$$

$$+ \frac{70}{269} ND_s \int_{12.2}^\infty \exp\left[-\frac{(h - 12.2)}{6.4} \right] dh$$

transforming the first integral by

$$\left(1 - \frac{h}{42.7} \right) = x$$

$$dh = -42.7\,dx$$

so that

$$\int \left(1 - \frac{h}{42.7} \right)^4 dh = -42.7 \int x^4\,dx$$

$$= -42.7 \frac{x^5}{5}$$

$$= -\frac{42.7}{5} \left[\left(1 - \frac{h}{42.7} \right)^5 \right]_0^{12.2}$$

$$= 6.952$$

Transforming the second integral by

$$-\frac{(h - 12.2)}{6.4} = x$$

$$dh = -6.4\,dx$$

so that

$$\int \exp\left[-\frac{(h-12.2)}{6.4}\right] dh = -6.4 \int \exp(x)\, dx$$

$$= -6.4 \exp(x)$$

$$= -6.4\left[\exp\left(-\frac{(h-12.2)}{6.4}\right)\right]_{12.2}^{\infty}$$

$$= 6.4$$

Or, finally

$$\int_0^\infty ND(h)\, dh = ND_s(6.952)$$

$$+ \frac{70}{269} ND_s(6.4)$$

$$= 8.6174(ND_s)$$

Performing the wet refractivity integration, one has

$$\int_0^\infty NW(h)\, dh = \int_0^{13} NW_s\left(1-\frac{h}{13}\right)^4 dh$$

$$= NW_s \int_0^{13}\left(1-\frac{h}{13}\right)^4 dh$$

Transforming the integral by

$$\left(1-\frac{h}{13}\right) = x$$

$$dh = -13\, dx$$

$$\int\left(1-\frac{h}{13}\right)^4 dh = -13 \int x^4\, dx$$

$$= -13\frac{x^5}{5}$$

$$= \frac{13}{5}\left[\left(1-\frac{h}{13}\right)^5\right]_0^{13}$$

$$= 2.6$$

so that

$$\int_0^\infty NW(h)\, dh = 2.6(NW_s)$$

Combining the integrated wet refractivity and the integrated dry refractivity yields

$$\frac{\int_0^\infty NW(h)\, dh}{\int_0^\infty ND(h)\, dh} = \frac{2.6(NW_s)}{8.6174(ND_s)}$$

$$= 0.30172\left(\frac{NW_s}{ND_s}\right)$$

This is to be compared to the previously determined relationship from actual data of:

$$\frac{\int_0^\infty NW(h)\, dh}{\int_0^\infty ND(h)\, dh} \approx 0.3224\left(\frac{NW_s}{ND_s}\right)$$

Since the value of the 1σ standard deviation

$$1\sigma = 00.93\% \ (\sim 2 \text{ cm})$$

found from actual data compares favorably with the most recent modeling published by Chao in Ref. 8 (~ 3 cm for combined night and day profiles), and since the basic relationship seems verifiable by average profiles presented by Chao; the determined expression will be adopted for use with the optical refraction model. The surface refractivity (Ref. 7) is defined as:

$$NW_s = \frac{(RH)_s C_1 C_2}{T_s^2}\exp\left(\frac{AT_s - B}{T_s - C}\right)$$

$$ND_s = C_1\frac{P_s}{T_s}$$

so that one would obtain

$$\left\{1 + \frac{\int_0^\infty NW(h)\, dh}{\int_0^\infty ND(h)\, dh}\right\} \cong 1 + (0.3224)\frac{(RH)_s C_2}{T_s P_s}\exp\left(\frac{AT_s - B}{T_s - C}\right)$$

To integrate this expression into the optical model, the pressure term must be converted from mbar to mm:

$$P_s(\text{mbar}) = P_s(\text{mm}) \times \frac{1013}{760}$$

so that one would finally have

$$\left\{1 + \frac{\int NW(h)\, dh}{\int ND(h)\, dh}\right\} \cong 1 + \frac{(7.1 \times 10^3)(RH)_s}{T_s P_s}\exp\left(\frac{AT_s - B}{T_s - C}\right)$$

where

$(RH)_s$ = surface relative humidity (100% = 1.0)

T_s = surface temperature, K

P_s = surface pressure, mm of Hg

$A = 17.149$

$B = 4684.1$

$C = 38.450$

D. Final Angular Tropospheric Radio Frequency Refraction Model

The following gives the complete radio frequency angular tropospheric refraction model:

$$R = F_p F_t F_w \left(\exp\left\{ \frac{\sum_{j=0}^{8} K_{j+3}[U(Z)]^j}{1 + \Delta_3(Z)} \right\} - K_{12} \right)$$

$$F_p = \left(\frac{P}{P_0} \left\{ 1 - \frac{\Delta_1(P,Z)}{1 + \Delta_3(Z)} \right\} \right)$$

$$F_t = \left(\frac{T_0}{T} \left\{ 1 - \frac{\Delta_2(T,Z)}{1 + \Delta_3(Z)} \right\} \right)$$

$$F_w = \left(1 + \frac{W_0 RH}{TP} \left\{ \exp\left[\frac{W_1 T - W_2}{T - W_3} \right] \right\} \right)$$

$$\Delta_1(P,Z) = (P - P_0)\{\exp[A_1(Z - A_2)]\}$$

$$\Delta_2(T,Z) = (T - T_0)\{\exp[B_1(Z - B_2)]\}$$

$$\Delta_3(Z) = (Z - C_0)\{\exp[C_1(Z - C_2)]\}$$

where

R = refraction, sec

Z = actual zenith angle, deg

EL = elevation angle

$EL = 90$ deg $- Z$

$U(Z) = \left\{ \dfrac{Z - K_1}{K_2} \right\}$

$K_1 = 46.625$

$K_2 = 45.375$

$K_3 = 4.1572$

$K_4 = 1.4468$

$K_5 = 0.25391$

$K_6 = 2.2716$

$K_7 = -1.3465$

$K_8 = -4.3877$

$K_9 = 3.1484$

$K_{10} = 4.5201$

$K_{11} = -1.8982$

$K_{12} = 0.89000$

P = pressure, mm Hg

$P_0 = 760.00$ mm Hg

$A_1 = 0.40816$

$A_2 = 112.30$

T = temperature, K

$T_0 = 273.00$ K

$B_1 = 0.12820$

$B_2 = 142.88$

$C_0 = 91.870$

$C_1 = 0.80000$

$C_2 = 99.344$

RH = Relative humidity (100% = 1.0)

$W_0 = 7.1 \times 10^3$

$W_1 = 17.149$

$W_2 = 4684.1$

$W_3 = 38.450$

E. Model Accuracies

The inaccuracies introduced by the wet refractivity term predominate over the inaccuracies presented in Section II. Considering

$$1\sigma = 1.00\%$$

the maximum 1σ angular errors would be

Z, deg	ΔR, sec	ΔR, deg
0–85	6	0.002
85–90	18	0.005
90–93	50	0.015

F. FORTRAN Subroutines of the Radio Frequency Refraction Models

Section II presented two FORTRAN subroutines, corresponding to the full optical refraction model and an abbreviated version. These two routines have been transformed to the radio frequency version of the refraction model, and are presented in Appendixes C and D. The FORTRAN subroutine SBEND (Appendix C) represents the full model, while XBEND (Appendix D) gives the abbreviated version. Inputs required are:

PRESS = pressure, mm of Hg

TEMP = temperature, K

HUMID = % of relative humidity (100% = 1.0)

ZNITH = actual zenith angle, deg

and the subroutines return with

R = refraction correction, sec

References

1. Garfinkel, B., "An Investigation in the Theory of Astronomical Refraction," *Astron. J.*, Vol. 50. No. 8. 1944.

2. Garfinkel, B., "Astronomical Refraction in a Polytropic Atmosphere," *Astron J.*, Vol. 72, No. 2, 1967.

3. Mueller, I. I., *Spherical and Practical Astronomy as Applied to Geodesy*, Frederick Ungar Publishing Co., New York, 1969.

4. Orlov, B. A., *Refraction Tables of Pulkova Observatory*, 4th Edition, 1956.

5. Lawson, C. L., "Least Squares Polynomial Fit to Data, S.P.," *JPL Fortran V Subroutine Directory*, 1846-23 (JPL internal document).

6. Chao, C. C., "New Tropospheric Range Corrections With Seasonal Adjustment" in *The Deep Space Network Progress Report*, No. 32-1526, Vol. VI, pp. 67–73, Jet Propulsion Laboratory, Pasadena, Calif., Dec. 15, 1971.

7. Berman, A. L., "A New Tropospheric Range Refraction Model" in *Space Programs Summary*, No. 37-65, Vol. II, pp. 140–153, Jet Propulsion Laboratory, Pasadena, Calif., Sept. 30, 1970.

8. Chao, C. C., "A New Method To Predict Wet Zenith Range Correction From Surface Measurements" in *The Deep Space Network Progress Report*, No. 32-1526, Vol. XIV, pp. 33–41, Jet Propulsion Laboratory, Pasadena, California, April 15, 1973.

Bibliography

Berman, A. L., *Adjustment of Predict Refraction Model to Prevent (Apparent) Lagrangian Interpolation Problems in Angle Predictions*, 401-2177, Aug. 13, 1971 (JPL internal document).

Rovello, R. C., *Antenna Pointing Subsystem Phase I, Computer Program, DSIF 210 ft Antennas*, 900-22, 315-R-6, Rev. 1, June 1967 (JPL internal document).

Smart, W. M., *Spherical Astronomy*, Cambridge University Press, London, 1965.

Table 1. Garfinkel refraction data[a] for P = 760 mm and T = 0°C

Z	R	R'	Z	R	R'	Z	R	R'
0.0	0.00	0.00	23.5	26.33	26.34	47.0	64.95	64.99
0.5	0.55	0.55	24.0	26.97	26.97	47.5	66.10	66.15
1.0	1.07	1.08	24.5	27.60	27.61	48.0	67.28	67.32
1.5	1.61	1.61	25.0	28.25	28.26	48.5	68.47	68.52
2.0	2.15	2.15	25.5	28.90	28.91	49.0	69.69	69.73
2.5	2.68	2.68	26.0	29.55	29.56	49.5	70.93	70.97
3.0	3.22	3.22	26.5	30.21	30.22	50.0	72.19	72.24
3.5	3.75	3.76	27.0	30.88	30.89	50.5	73.48	73.53
4.0	4.29	4.29	27.5	31.55	31.56	51.0	74.79	74.85
4.5	4.83	4.83	28.0	32.23	32.24	51.5	76.14	76.19
5.0	5.36	5.36	28.5	32.91	32.92	52.0	77.51	77.57
5.5	5.90	5.90	29.0	33.60	33.62	52.5	78.91	78.97
6.0	6.43	6.44	29.5	34.30	34.32	53.0	80.34	80.40
6.5	6.97	6.97	30.0	35.01	35.02	53.5	81.80	81.87
7.0	7.51	7.51	30.5	35.72	35.73	54.0	83.30	83.37
7.5	8.05	8.05	31.0	36.43	36.45	54.5	84.83	84.91
8.0	8.59	8.59	31.5	37.16	37.17	55.0	86.40	86.48
8.5	9.12	9.13	32.0	37.89	37.91	55.5	88.02	88.10
9.0	9.67	9.67	32.5	38.63	38.65	56.0	89.68	89.77
9.5	10.21	10.21	33.0	39.38	39.40	56.5	91.39	91.48
10.0	10.75	10.75	33.5	40.14	40.16	57.0	93.14	93.23
10.5	11.30	11.30	34.0	40.90	40.92	57.5	94.94	95.03
11.0	11.84	11.84	34.5	41.68	41.70	58.0	96.78	96.88
11.5	12.39	12.39	35.0	42.46	42.48	58.5	98.67	98.78
12.0	12.94	12.94	35.5	43.26	43.27	59.0	100.61	100.72
12.5	13.49	13.49	36.0	44.06	44.08	59.5	102.61	102.72
13.0	14.04	14.05	36.5	44.87	44.89	60.0	104.66	104.78
13.5	14.60	14.60	37.0	45.69	45.71	60.5	106.76	106.89
14.0	15.15	15.16	37.5	46.53	46.55	61.0	108.93	109.06
14.5	15.71	15.72	38.0	47.37	47.39	61.5	111.17	111.31
15.0	16.28	16.28	38.5	48.23	48.25	62.0	113.49	113.64
15.5	16.84	16.85	39.0	49.10	49.12	62.5	115.93	116.10
16.0	17.41	17.41	39.5	49.98	50.00	63.0	118.47	118.64
16.5	17.98	17.98	40.0	50.87	50.89	63.5	121.10	121.28
17.0	18.55	18.56	40.5	51.77	51.80	64.0	123.79	123.98
17.5	19.13	19.13	41.0	52.69	52.72	64.5	126.53	126.72
18.0	19.70	19.71	41.5	53.62	53.65	65.0	129.35	129.56
18.5	20.29	20.29	42.0	54.56	54.59	65.5	132.28	132.50
19.0	20.87	20.88	42.5	55.52	55.55	66.0	135.33	135.57
19.5	21.46	21.47	43.0	56.50	56.53	66.5	138.51	138.76
20.0	22.06	22.06	43.5	57.49	57.52	67.0	141.82	142.09
20.5	22.65	22.66	44.0	58.50	58.53	67.5	145.26	145.55
21.0	23.26	23.66	44.5	59.52	59.56	68.0	148.86	149.17
21.5	23.86	23.87	45.0	60.56	60.60	68.5	152.64	152.97
22.0	24.47	24.48	45.5	61.63	61.67	69.0	156.61	156.97
22.5	25.09	25.09	46.0	62.72	62.76	69.5	160.75	161.13
23.0	25.71	25.72	46.5	63.83	63.87	70.0	165.06	165.46

[a]R gives the refraction correction if Z = actual while R' gives the refraction correction if Z = observed.

Table 1 (contd)

Z	R	R'	Z	R	R'	Z	R	R'
70.2	166.83	167.25	79.8	323.92	326.68	87.2	895.71	947.24
70.4	168.63	169.06	80.0	330.09	333.02	87.3	914.73	969.38
70.6	170.47	170.91	80.2	336.46	339.52	87.4	934.45	992.51
70.8	172.33	172.78	80.4	342.99	346.20	87.5	954.84	1016.58
71.0	174.23	174.69	80.6	349.75	353.18	87.6	975.96	1041.62
71.2	176.16	176.64	80.8	356.81	360.45	87.7	997.91	1067.68
71.4	178.13	178.63	81.0	364.17	368.05	87.8	1020.64	1095.01
71.6	180.15	180.66	81.2	371.82	375.93	87.9	1044.16	1123.53
71.8	182.20	182.73	81.4	379.76	384.12	88.0	1068.53	1153.28
72.0	184.30	184.85	81.6	387.99	392.61	88.1	1093.93	1184.47
72.2	186.44	187.01	81.8	396.55	401.48	88.2	1120.27	1217.10
72.4	188.64	189.23	82.0	405.48	410.74	88.3	1147.59	1251.29
72.6	190.90	191.51	82.2	414.76	420.35	88.4	1176.01	1287.15
72.8	193.21	193.84	82.4	424.44	430.45	88.5	1205.55	1324.68
73.0	195.57	196.22	82.6	434.59	441.05	88.6	1236.25	1364.16
73.2	197.97	198.64	82.8	445.21	452.12	88.7	1268.19	1405.55
73.4	200.41	201.10	83.0	456.30	463.71	88.8	1301.38	1449.01
73.6	202.90	203.62	83.2	467.87	475.82	88.9	1335.90	1494.78
73.8	205.45	206.19	83.4	480.03	488.71	89.0	1371.84	1543.13
74.0	208.07	208.84	83.6	492.90	502.21	89.1	1409.18	1594.01
74.2	210.75	211.56	83.8	506.32	516.28	89.2	1448.01	1647.64
74.4	213.51	214.35	84.0	520.31	531.10	89.3	1488.47	1704.25
74.6	216.34	217.20	84.2	535.04	546.76	89.4	1530.70	1764.12
74.8	219.23	220.12	84.4	550.57	563.28	89.5	1574.66	1827.44
75.0	222.18	223.11	84.6	566.91	580.76	89.6	1620.40	1894.34
75.2	225.21	226.18	84.8	584.18	599.35	89.7	1668.02	1965.25
75.4	228.33	229.34	85.0	602.50	619.11	89.8	1717.65	2040.56
75.6	231.54	232.60	85.1	612.07	629.38	89.9	1769.36	2123.12
75.8	234.84	235.94	85.2	621.88	639.99	90.0	1823.24	2205.54
76.0	238.20	239.34	85.3	631.94	650.89	90.1	1879.28	2298.34
76.2	241.64	242.81	85.4	642.32	662.10	90.2	1937.63	2392.18
76.4	245.15	246.37	85.5	652.95	673.70	90.3	1998.35	2495.00
76.6	248.77	250.05	85.6	663.88	685.73	90.4	2062.49	2604.75
76.8	252.50	253.85	85.7	675.18	698.15	90.5	2130.07	2722.08
77.0	256.35	257.75	85.8	686.86	710.99	90.6	2196.81	2847.58
77.2	260.29	261.74	85.9	698.89	724.30	90.7	2269.53	2982.06
77.4	264.33	265.85	86.0	711.31	738.00	90.8	2343.68	3126.84
77.6	268.50	270.10	86.1	724.15	752.11	90.9	2419.93	3282.69
77.8	272.80	274.48	86.2	737.33	766.87	91.0	2500.71	3450.46
78.0	277.24	279.00	86.3	750.87	782.12	91.1	2584.52	3632.11
78.2	281.80	283.63	86.4	764.99	797.78	91.2	2671.66	3827.51
78.4	286.49	288.41	86.5	779.57	814.09	91.3	2762.19	4039.04
78.6	291.32	293.34	86.6	794.50	831.04	91.4	2856.17	4269.13
78.8	296.33	298.45	86.7	809.95	848.62	91.5	2953.70	4519.72
79.0	301.50	303.73	86.8	825.98	866.83	91.6	3055.07	4792.26
79.2	306.85	309.20	86.9	842.56	885.73	91.7	3160.32	5090.87
79.4	312.36	314.82	87.0	859.68	905.41	91.8	3269.46	5418.31
79.6	318.03	320.62	87.1	877.38	925.93	91.9	3382.48	5777.87

Table 1 (contd)

Z	R	R'
92.0	3499.59	6174.23
92.1	3621.06	6612.15
92.2	3746.26	7097.56
92.3	3875.53	7638.78
92.4	4009.10	8246.36
92.5	4147.07	8926.70
92.6	4289.48	9692.48
92.7	4436.33	10560.24
92.8	4587.50	11551.26
92.9	4742.84	12684.70
93.0	4902.77	13986.89

Table 2. Maximum refraction model residuals for selected P, T, and ranges of Z

Temperature, °C	Maximum refraction model residuals, sec		
	$P = 700$	$P = 760$	$P = 800$
a. $0° \leq Z \leq 85°$			
−10	+4.59	+4.87	+5.05
0	+5.25	+5.59	+5.82
+10	+5.83	+6.24	+6.51
+20	+6.41	+6.88	+7.18
+30	+6.98	+7.50	+7.83
b. $85° \leq Z < 93°$			
−10	−15.41	−18.36	−24.30
0	−13.56	−15.03	−17.45
+10	−11.91	−14.27	−14.02
+20	−15.16	−14.77	−12.61
+30	−19.20	−16.20	+13.94

Table 3. Maximum refraction model residuals for selected P, T, and ranges of Z: Δ_1, Δ_2, $\Delta_3 = 0$

Temperature, °C	Maximum refraction model residuals, sec		
	$P = 700$	$P = 760$	$P = 800$
a. $0° \leq Z \leq 85°$			
−10	+6.06	+6.38	+6.57
0	+5.33	+5.61	+5.78
+10	+4.68	+4.93	+5.08
+20	+4.11	+4.32	+4.45
+30	+3.59	−5.41	−6.06
b. $85° \leq Z < 93°$			
−10	+102.05	−188.07	−278.89
0	−130.49	−251.98	−338.33
+10	−196.42	−312.90	−395.56
+20	−258.65	−370.69	−450.09
+30	−317.28	−452.40	−501.90

Table 4. Surface refractivity vs integrated refractivity: A = 0.3224; σ = 0.93%

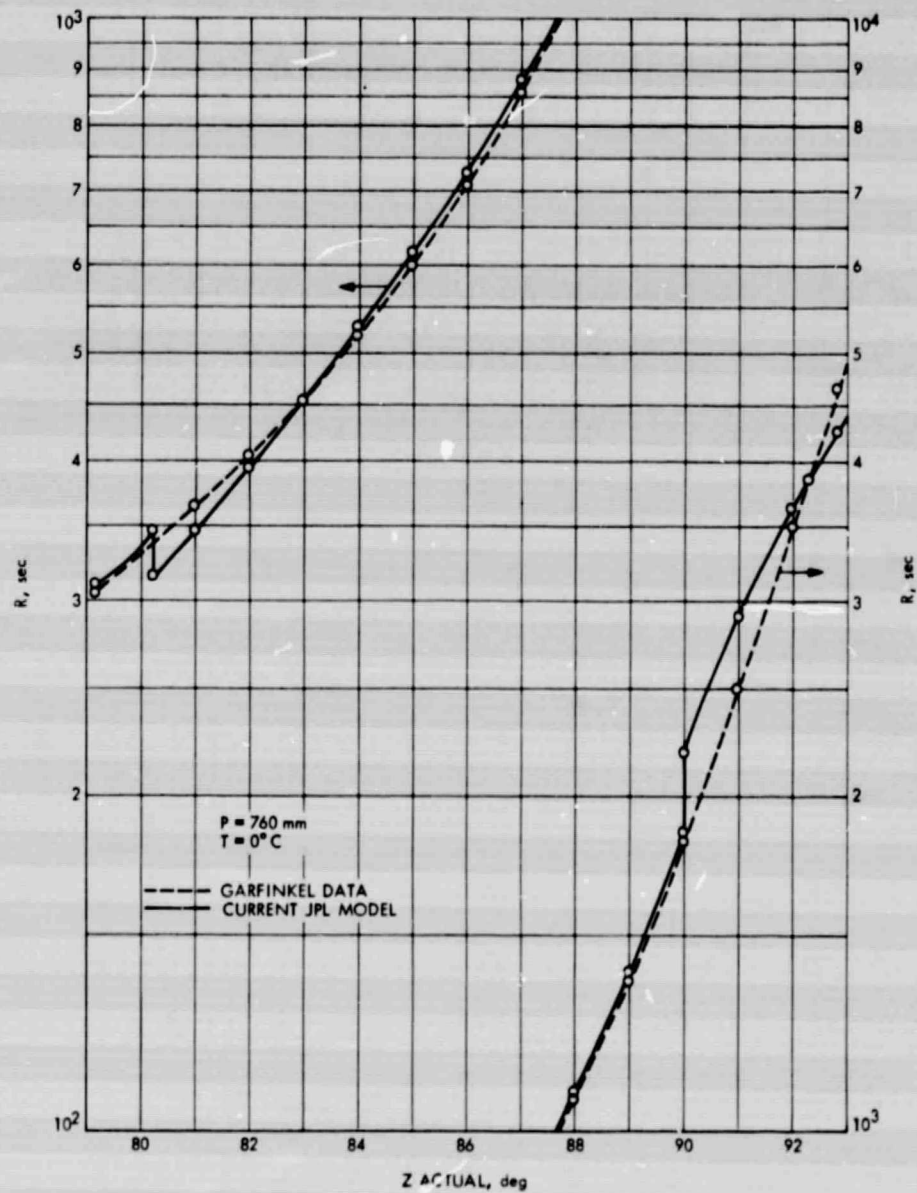| Case	$100 \times \dfrac{NW_s}{ND_s}$ (%)	$A \times \left\{ 100 \times \dfrac{NW_s}{ND_s} \right\}$ (%)	$100 \times \dfrac{\int NW(h)\,dh}{\int ND(h)\,dh}$ (%)	Δ (%)	Δ, cm
1	4.86	1.57	2.27	+0.70	+1.48
2	3.76	1.21	2.17	+0.96	+2.03
3	5.74	1.85	1.80	−0.05	−0.11
4	5.34	1.72	1.37	−0.35	−0.74
5	4.74	1.53	1.75	+0.22	+0.47
6	7.14	2.30	2.17	−0.13	−0.28
7	24.11	7.77	8.55	+0.78	+1.65
8	31.72	10.23	9.12	−1.11	−2.35
9	7.29	2.35	4.58	+2.23	+4.72
10	9.89	3.19	2.69	−0.50	−1.06

Fig. 1. Current 3-segment JPL angular refraction model vs Garfinkel refraction data
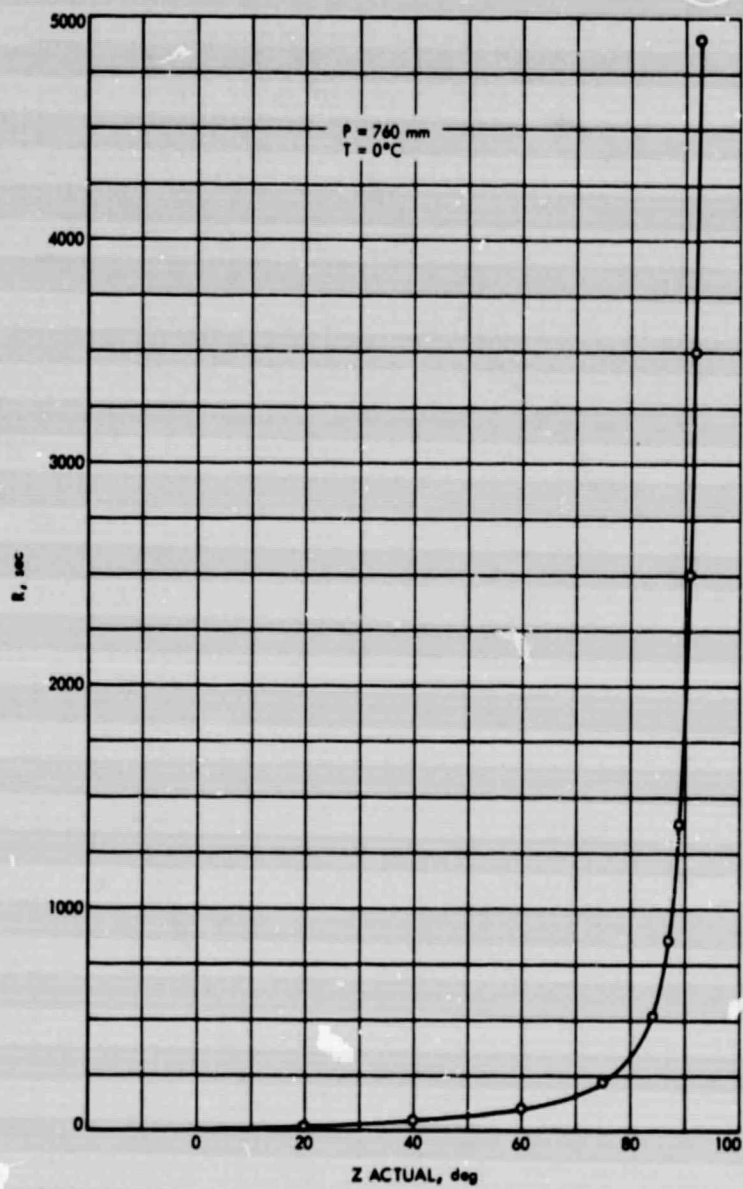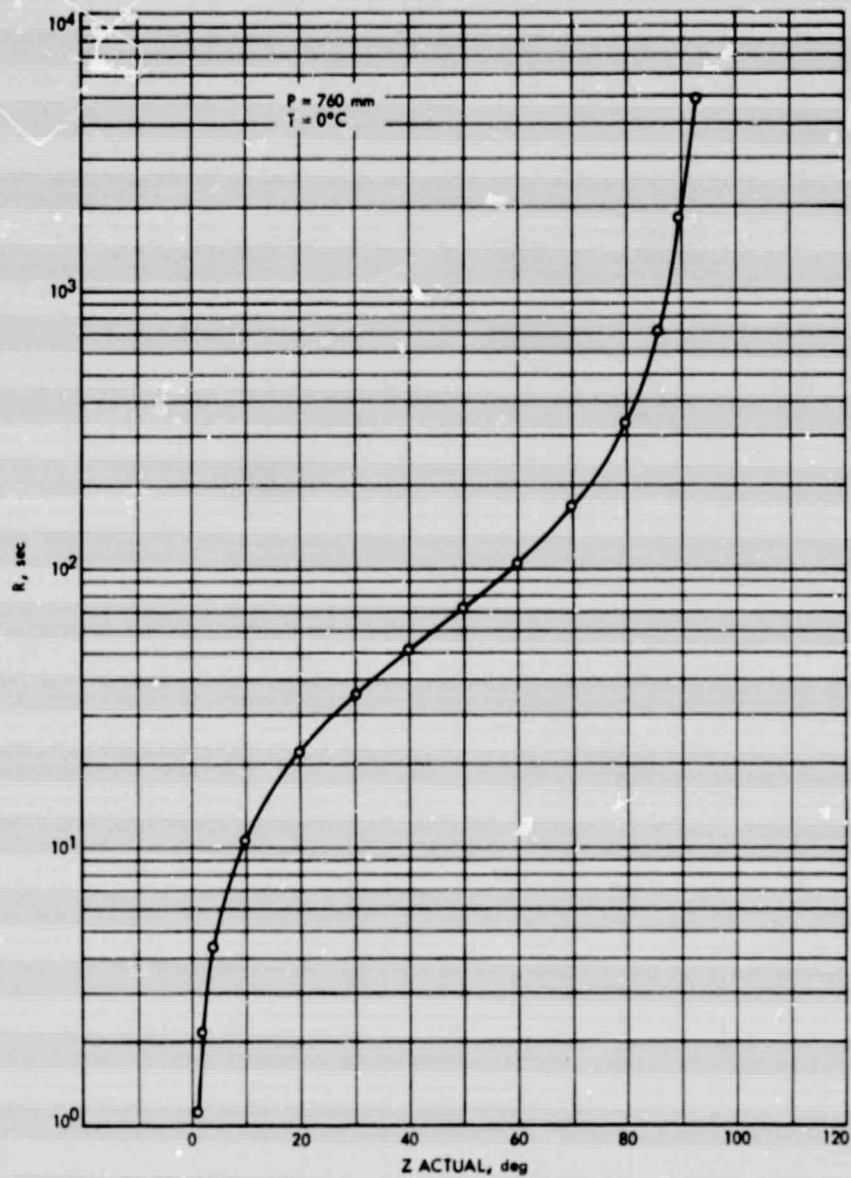
Fig. 2. Garfinkel refraction data

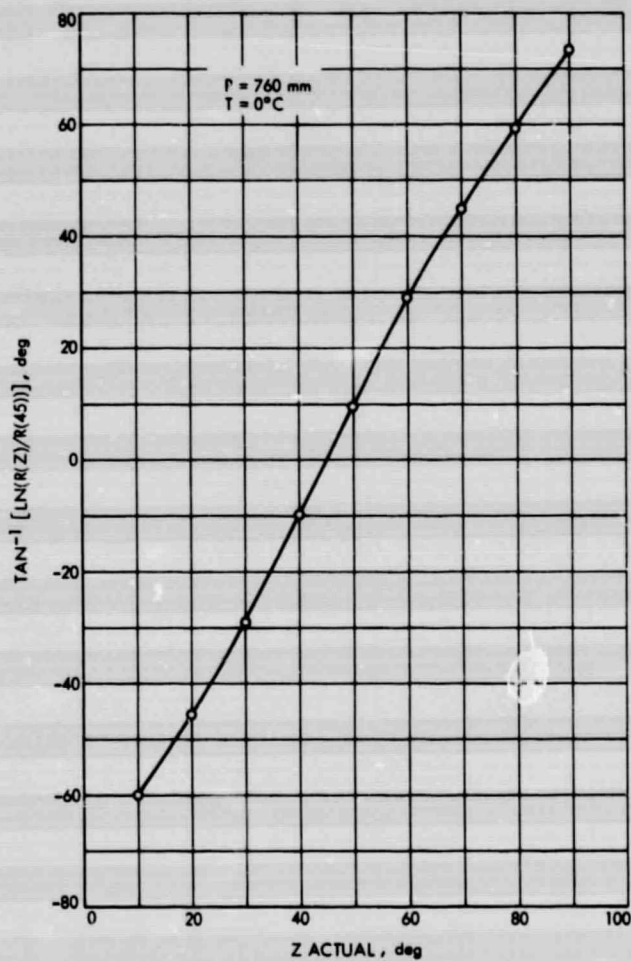Fig. 3. Garfinkel refraction data (logarithmic)

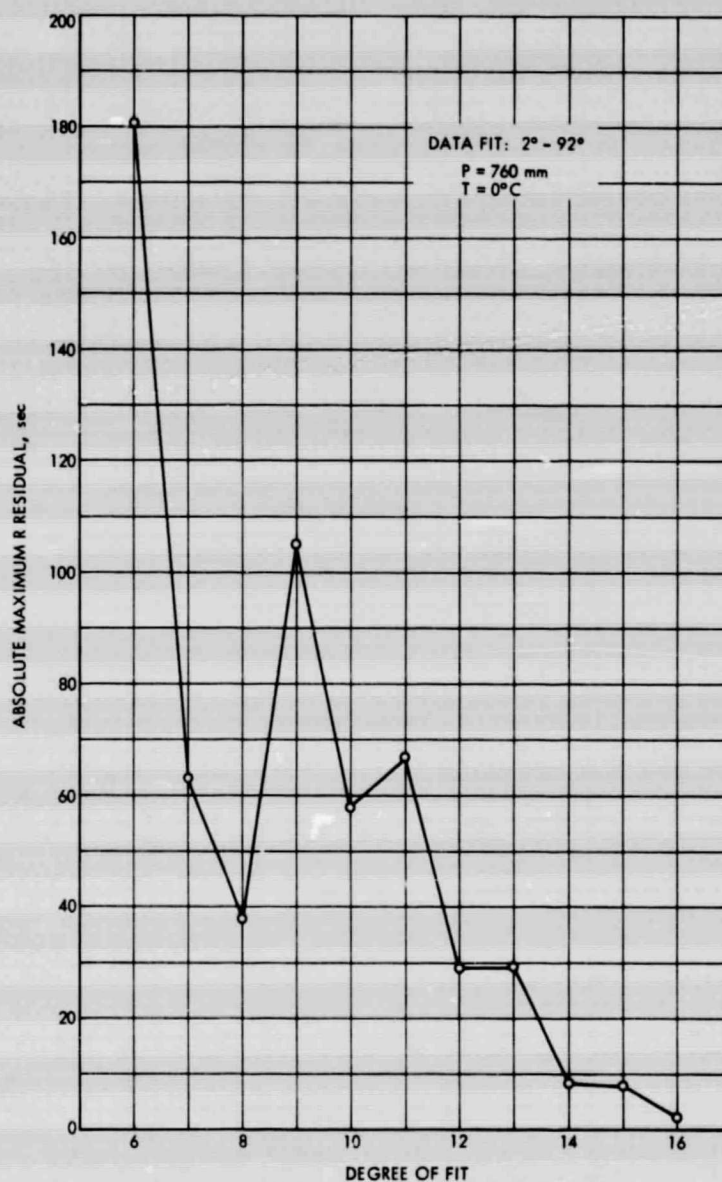Fig. 4. Garfinkel refraction data (arctan (ln R))

Fig. 5. Least squares fit of ln R (Garfinkel data) to an nth degree polynomial
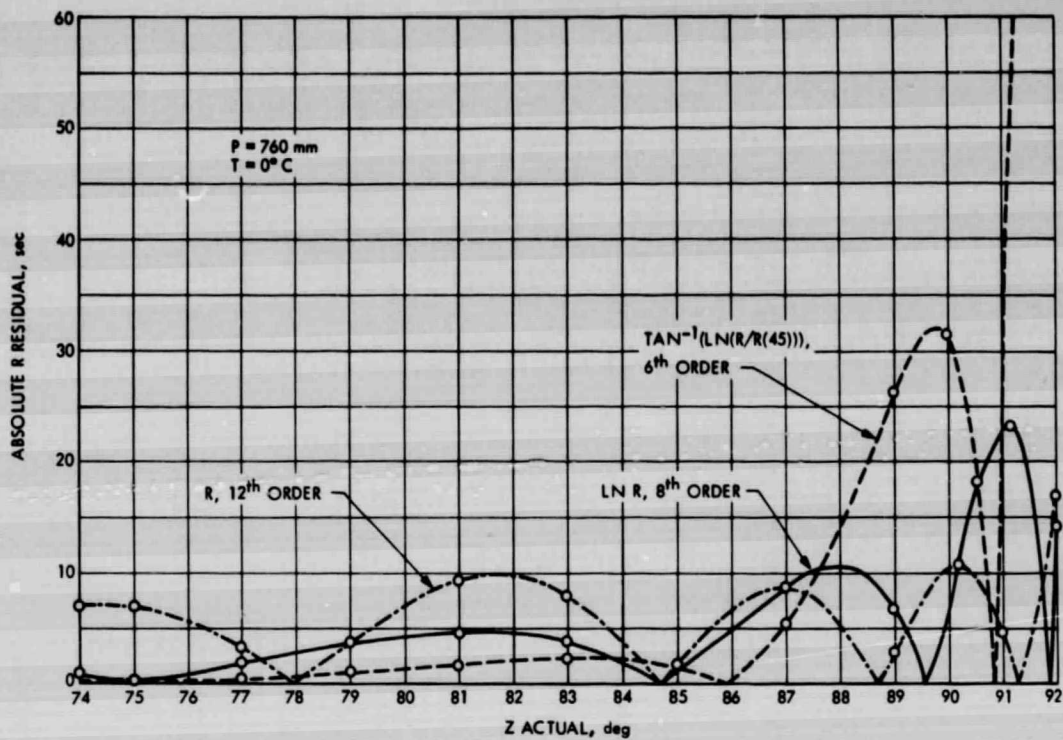
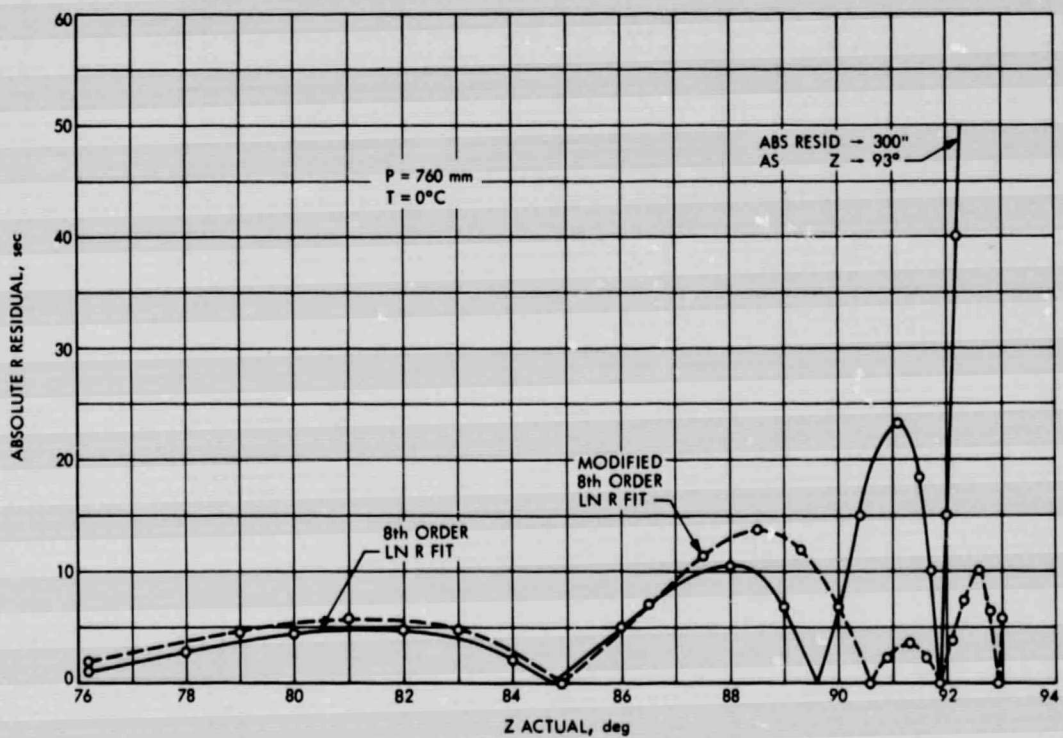Fig. 6. Various functional forms of *R* fit to an *n*th degree polynomial

Fig. 7. 8th degree and modified 8th degree polynomial fit to ln *R* (Garfinkel data)
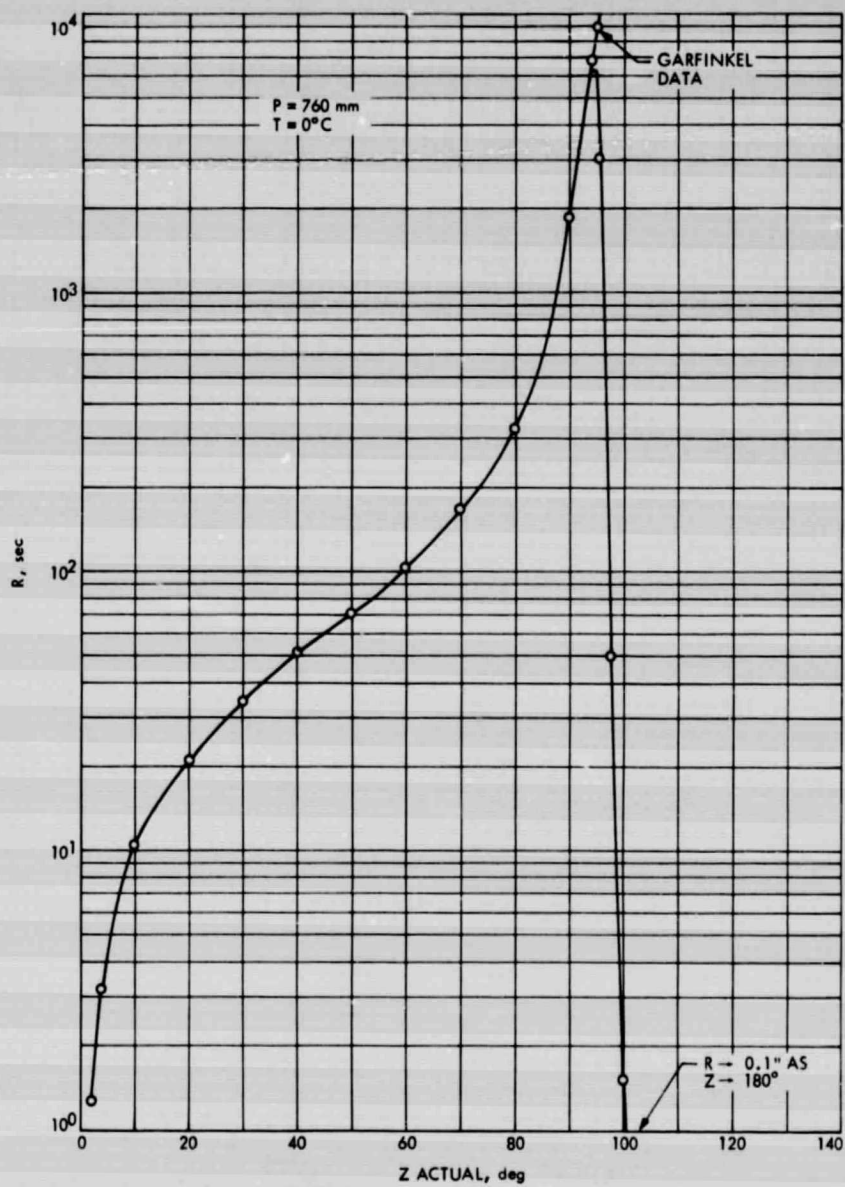
Fig. 8. Berman-Rockwell refraction model
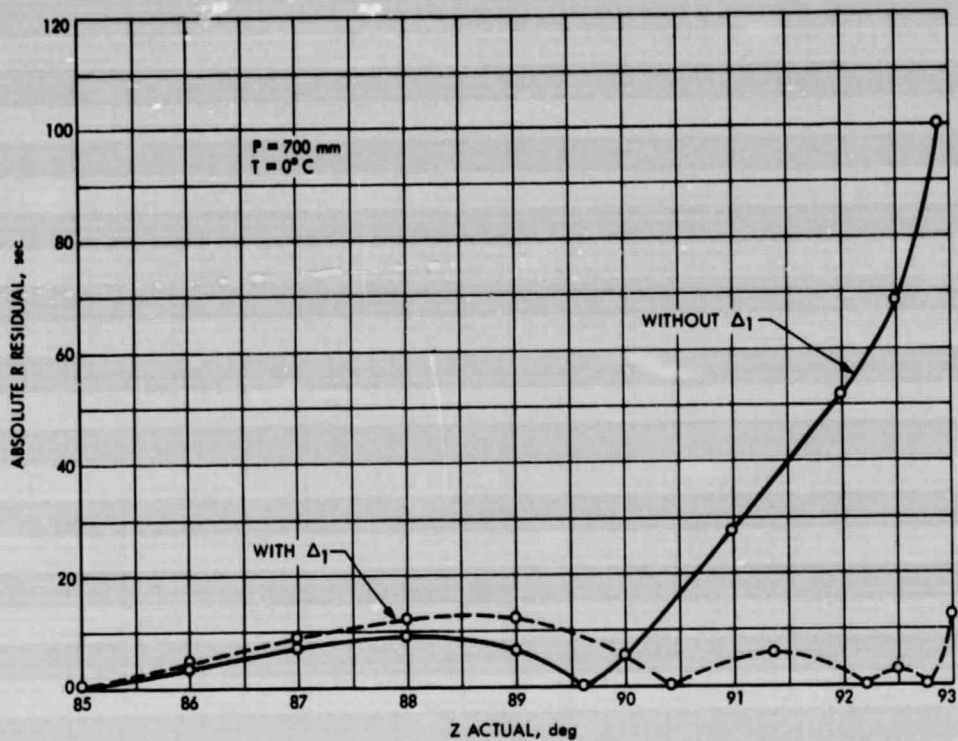
Fig. 9. Refraction model with and without Δ_1 (pressure correction factor)
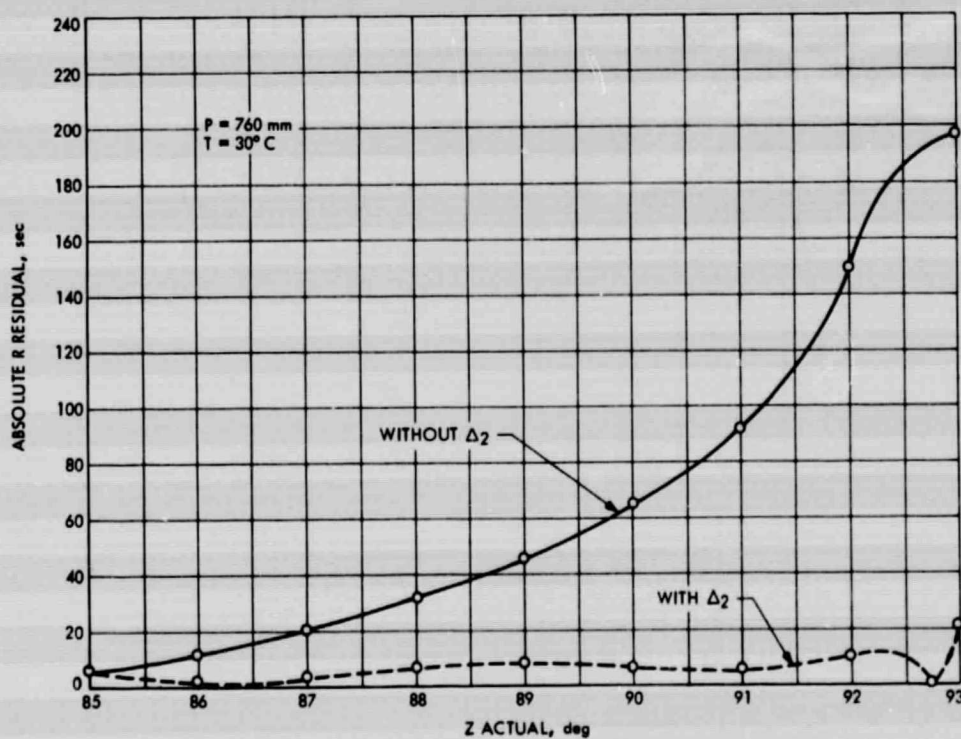

Fig. 10. Refraction model with and without Δ_2 (temperature correction factor)
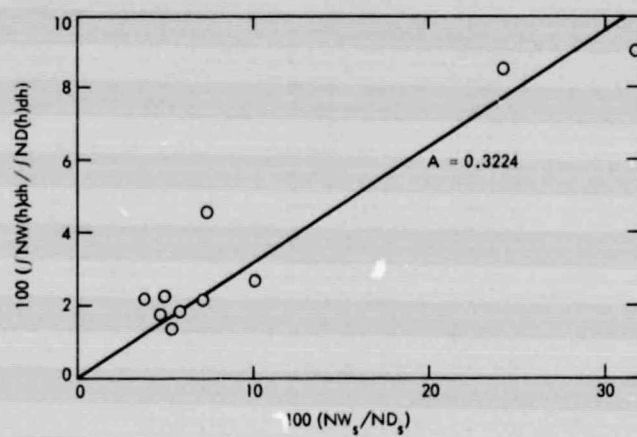
Fig. 11. Integrated refractivity vs surface refractivity

Appendix A

Subroutine BEND I

```
00101      1*           SUBROUTINE BEND(PRESS,TEMP,ZNITH,R)
00103      2*           DIMENSION A(2),B(2),C(2),E(12),P(2),T(2),Z(2)
00104      3*           P(1) = 760.00
00105      4*           P(2) = PRESS
00106      5*           T(1) = 273.00
00107      6*           T(2) = TEMP
00110      7*           Z(1) = 91.870
00111      8*           Z(2) = ZNITH
00112      9*           A(1) = .40816
00113     10*           A(2) = 112.30
00114     11*           B(1) = .12820
00115     12*           B(2) = 142.88
00116     13*           C(1) = .80000
00117     14*           C(2) = 99.344
00120     15*           E(1) = 46.625
00121     16*           E(2) = 45.375
00122     17*           E(3) = 4.1572
00123     18*           E(4) = 1.4468
00124     19*           E(5) = .25391
00125     20*           E(6) = 2.2716
00126     21*           E(7) =-1.3465
00127     22*           E(8) =-4.3877
00130     23*           E(9) = 3.1484
00131     24*           E(10)= 4.5201
00132     25*           E(11)=-1.8982
00133     26*           E(12)= .89000
00134     27*           D3=1.+DELTA(Z,C,Z(2))
00135     28*           FP=(P(2)/P(1))*(1.-DELTA(P,A,Z(2))/D3)
00136     29*           FT=(T(1)/T(2))*(1.-DELTA(T,B,Z(2))/D3)
00137     30*           U=(Z(2)-E(1))/E(2)
00140     31*           X=E(11)
00141     32*           DO 1 I=1,8
00144     33*         1 X=E(11-I)+U*X
00146     34*           R=FT*FP*(EXP(X/D3)-E(12))
00147     35*           RETURN
00150     36*           END


00101      1*           FUNCTION DELTA(A,B,Z)
00103      2*           DIMENSION A(2),B(2)
00104      3*           DELTA=(A(2)-A(1))*EXP(B(1)*(Z-B(2)))
00105      4*           RETURN
00106      5*           END
```

Appendix B

Subroutine BEND II

```
00101    1*           SUBROUTINE BEND(PRESS,TEMP,ZNITH,R)
00103    2*           DIMENSION E(12)
00104    3*           P    = 760.00
00105    4*           T    = 273.00
00106    5*           E(1) = 46.625
00107    6*           E(2) = 45.375
00110    7*           E(3) = 4.1572
00111    8*           E(4) = 1.4468
00112    9*           E(5) = .25391
00113   10*           E(6) = 2.2716
00114   11*           E(7) =-1.3465
00115   12*           E(8) =-4.3877
00116   13*           E(9) = 3.1484
00117   14*           E(10)= 4.5201
00120   15*           E(11)=-1.8982
00121   16*           E(12)= .89000
00122   17*           FP=PRESS/P
00123   18*           FT=T/TEMP
00124   19*           U=(ZNITH-E(1))/E(2)
00125   20*           X=E(11)
00126   21*           DO 1 I=1,8
00131   22*         1 X=E(11-I)+U*X
00133   23*           R=FT*FP*(EXP(X)-E(12))
00134   24*           RETURN
00135   25*           END
```

Appendix C

Subroutine SBEND

```
00101      1*          SUBROUTINE SBEND(PRESS,TEMP,HUMID,ZNITH,R)
00103      2*          DIMENSION A(2),B(2),C(2),E(12),P(2),T(2),Z(2)
00104      3*          P(1) = 760.00
00105      4*          T(1) = 273.00
00106      5*          Z(1) = 91.870
00107      6*          P(2) = PRESS
00110      7*          T(2) = TEMP
00111      8*          Z(2) = ZNITH
00112      9*          A(1) = .40816
00113     10*          A(2) = 112.30
00114     11*          B(1) = .12820
00115     12*          B(2) = 142.88
00116     13*          C(1) = .80000
00117     14*          C(2) = 99.344
00120     15*          E(1) = 46.625
00121     16*          E(2) = 45.375
00122     17*          E(3) = 4.1572
00123     18*          E(4) = 1.4468
00124     19*          E(5) = .25391
00125     20*          E(6) = 2.2716
00126     21*          E(7) =-1.3465
00127     22*          E(8) =-4.3877
00130     23*          E(9) = 3.1484
00131     24*          E(10)= 4.5201
00132     25*          E(11)=-1.8982
00133     26*          E(12)= .89000
00134     27*          W0   = 7100.0
00135     28*          W1   = 17.149
00136     29*          W2   = 4684.1
00137     30*          W3   = 38.450
00140     31*          D3=1.+DELTA(Z,C,Z(2))
00141     32*          FP=(P(2)/P(1))*(1.-DELTA(P,A,Z(2))/D3)
00142     33*          FT=(T(1)/T(2))*(1.-DELTA(T,B,Z(2))/D3)
00143     34*          FW=1+(W0*HUMID*EXP((W1*T(2)-W2)/(T(2)-W3))/(T(2)*P(2)))
00144     35*          U=(Z(2)-E(1))/E(2)
00145     36*          X=E(11)
00146     37*          DO 1 I=1,8
00151     38*       1  X=E(11-I)+U*X
00153     39*          R=FT*FP*FW*(EXP(X/D3)-E(12))
00154     40*          RETURN
00155     41*          END


00101      1*          FUNCTION DELTA(A,B,Z)
00103      2*          DIMENSION A(2),B(2)
00104      3*          DELTA=(A(2)-A(1))*EXP(B(1)*(Z-B(2)))
00105      4*          RETURN
00106      5*          END
```

Appendix D
Subroutine XBEND

```
00101    1.        SUBROUTINE XBEND(PRESS,TEMP,HUMID,ZNITH,R)
00103    2.        DIMENSION E(12)
00104    3.        P      = 760.00
00105    4.        T      = 273.00
00106    5.        E(1)  = 46.625
00107    6.        E(2)  = 45.375
00110    7.        E(3)  = 4.1572
00111    8.        E(4)  = 1.4468
00112    9.        E(5)  = .25391
00113   10.        E(6)  = 2.2714
00114   11.        E(7)  =-1.3465
00115   12.        E(8)  =-4.3877
00116   13.        E(9)  = 3.1484
00117   14.        E(10)= 4.5201
00120   15.        E(11)=-1.8982
00121   16.        E(12)= .89000
00122   17.        W0      = 7100.0
00123   18.        W1      = 17.149
00124   19.        W2      = 4684.1
00125   20.        W3      = 38.450
00126   21.        FP=PRESS/P
00127   22.        FT=T/TEMP
00130   23.        FW=1+W0*HUMID*EXP((W1*TEMP-W2)/(TEMP-W3))/(TEMP*PRESS)
00131   24.        U=(ZNITH-E(1))/E(2)
00132   25.        X=E(11)
00133   26.        DO 1 I=1,8
00136   27.      1 X=E(11-I)+U*X
00140   28.        R=FT*FP*FW*(EXP(X)-E(12))
00141   29.        RETURN
00142   30.        END
```